

Contact terms in $\gamma\gamma \rightarrow A_2\pi \rightarrow \rho\pi\pi$ transitions

E. Bagan, A. Bramon, and F. Cornet

Departament de Física Teòrica, Universitat Autònoma de Barcelona, Bellaterra, Barcelona, Spain

(Received 16 September 1982; revised manuscript received 20 December 1982)

The contribution of contact terms (originated by gauge invariance) to the $\gamma\gamma \rightarrow A_2^\pm \pi^\mp \rightarrow \rho^0 \pi^+ \pi^-$ transitions is evaluated. Large cross sections are predicted immediately above threshold.

The large values for $\sigma(\gamma\gamma \rightarrow \pi^+ \pi^- \pi^+ \pi^-)$ originally observed at PETRA (TASSO detector¹) and at SPEAR² have recently been confirmed³ by other groups and—with enlarged statistics—by the same authors. The sets of data are reasonably compatible and all of them present a peak for the cross section,

$$\sigma(\gamma\gamma \rightarrow \pi^+ \pi^- \pi^+ \pi^-) \simeq 100 \text{ nb} ,$$

at center-of-mass energies $W_{\gamma\gamma} \simeq 1.6 \text{ GeV}$. The reaction is found to be dominated by the

$$\gamma\gamma \rightarrow \rho^0 \rho^0 \rightarrow \pi^+ \pi^- \pi^+ \pi^-$$

channel but there seem to be significant differences between those groups concerning the $\rho^0 \rho^0$ signal.³ Theoretically, one has attributed this structure to the formation of a new $J^{PC} = 2^{-+}$ resonance,⁴ a glueball,⁵ or a $q\bar{q}q\bar{q}$ bound state.⁶ However, the large value of the width required by the most recent set of data and the shape of the structure seems to be more characteristic of a threshold effect rather than a genuine resonance.³

The purpose of this paper consists in considering the contribution to the four-charged-pion final state proceeding through the chain

$$\gamma\gamma \rightarrow A_2^\pm \pi^\mp \rightarrow \rho^0 \pi^+ \pi^- \rightarrow \pi^+ \pi^- \pi^+ \pi^- , \quad (1)$$

assuming that the first step is dominated by an electromagnetic contact term or point interaction analogous to that responsible for large threshold effects in other photon-initiated reactions.^{7,8} One expects a rapid growth of the cross section just above threshold, $W_{\gamma\gamma} = 1.45 \text{ GeV}$, due to the opening of the phase space and the s -wave nature of this contact term, followed by a suppression due to absorption.⁷ On the other hand, there is always one on-shell ρ^0 meson formed by one of the two $\pi^+ \pi^-$ pairs appearing in the final step of the chain (1), while for kinematical reasons the invariant mass of the remaining $\pi^+ \pi^-$ pair is found to be not far from m_ρ , thus simulating a $\rho^0 \rho^0$ signal for $W_{\gamma\gamma} \simeq 1.6 \text{ GeV}$.

The contact term initiating the chain (1) is generated by introducing covariant derivatives in the phenomenological Lagrangian accounting for the $A_2^\pm \rightarrow \pi^\pm \gamma$ transition. From the usual expression for

this $A_2 \rightarrow \pi\gamma$ matrix element,⁹

$$T(A_2 \rightarrow \pi\gamma) = -g \epsilon_{\alpha\beta\gamma\delta} \epsilon'^{\alpha} k'^{\beta} q^{\gamma} \epsilon^{\delta\lambda} k_{\lambda}^{\prime} , \quad (2)$$

one immediately deduces the contact term corresponding to the $\gamma\gamma \rightarrow A_2^\pm \pi^\mp$ amplitude,

$$T_{CT} = eg \epsilon_{\alpha\beta\gamma\delta} \epsilon'^{\alpha} k'^{\beta} \epsilon^{\gamma} \epsilon^{\delta\lambda} k_{\lambda}^{\prime} , \quad (3)$$

where $\epsilon^{\delta\lambda}$, ϵ^{λ} , and ϵ'^{α} (p , k , and k') are the polarization (four-momenta) of the A_2 meson and the photons, and q is the four-momentum of the pion. Notice that g^2 can be deduced (see below) from the data¹⁰ on $\Gamma(A_2 \rightarrow \pi\gamma)$ or $\Gamma(A_2 \rightarrow \rho\pi)$ [using vector-meson dominance (VMD) in the latter case] in such a way that no free parameters appear in our computation.

As is well known, the contact amplitude T_{CT} , Eq. (3), is only one term [corresponding to Fig. 1(a)] of the whole gauge-invariant amplitude T describing the

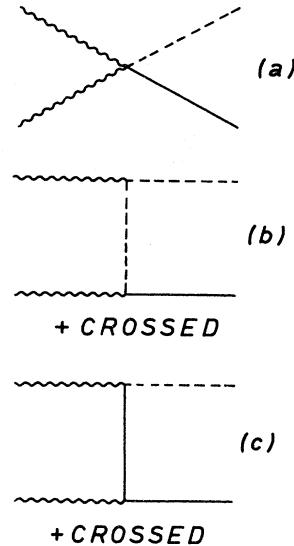


FIG. 1. (a)–(c) Gauge-invariant set of diagrams for $\gamma(k) + \gamma(k') \rightarrow A_2^\pm(p) + \pi^\mp(q)$. Wavy, dashed, and solid lines correspond to photons, pions, and A_2 mesons, respectively. Crossed diagrams are required by Bose statistics.

$\gamma\gamma \rightarrow A_2^\pm \pi^\mp$ transition. The other terms [Fig. 1(b) and 1(c)] are given by

$$T_\pi = -eg \frac{\epsilon \cdot (2q - k)}{2k \cdot q} \epsilon_{\alpha\beta\gamma\delta} \epsilon'^{\alpha} k'^{\beta} p^\gamma \epsilon^{\delta\lambda} k'_\lambda, \quad (4)$$

$$T_A = -eg \frac{\epsilon \cdot (2p - k)}{2k \cdot p} \epsilon_{\alpha\beta\gamma\delta} \epsilon'^{\alpha} k'^{\beta} q^\gamma \epsilon^{\delta\lambda} k'_\lambda \quad (5)$$

and contain the propagators of a π or an A_2 meson, respectively. At threshold, $W_{\gamma\gamma} = m_\pi + m_{A_2}$, the denominator of Eq. (5) turns out to be much larger than that corresponding to pion exchange,

$$2k \cdot p = m_{A_2} W_{\gamma\gamma} \gg m_\pi W_{\gamma\gamma} = 2k \cdot q,$$

and the contribution of T_A to the total amplitude is much smaller than that of T_π and almost negligible for the whole range of energies. For this reason, the $A_2 A_2 \gamma$ vertex and the A_2 polarization sum have been taken in the simplest form ("orbital current" part⁸) compatible with the required gauge invariance of $T = T_{CT} + T_\pi + T_A$ for both photons.

Taking Bose symmetry into account one obtains our final amplitude for the $\gamma\gamma \rightarrow A_2^\pm \pi^\mp$ transitions,

$$A \equiv A(\gamma\gamma \rightarrow A_2^\pm \pi^\mp) \\ = T(k, \epsilon, k', \epsilon') + T(k', \epsilon', k, \epsilon). \quad (6)$$

The differential cross section for the sum of both charge states is given by

$$\frac{d\sigma(\gamma\gamma \rightarrow A_2\pi)}{d\Omega} = \frac{1}{16\pi^2} \frac{1}{4} \sum |A|^2 \frac{|\vec{q}|}{W_{\gamma\gamma}^3}, \quad (7)$$

where the sum extends to all polarizations of the initial photons and final A_2 .

We now proceed to fix the value of the coupling constant g defined in Eq. (2) and appearing in the final cross section (7) through Eqs. (4)–(6). From the $A_2 \rightarrow \pi\gamma$ amplitude (2) one immediately obtains

$$\Gamma(A_2 \rightarrow \pi\gamma) = g^2 |\vec{p}|^5 / 40\pi,$$

where $|\vec{p}| = 0.65$ GeV is the final three-momentum. Then, the experimental value¹⁰

$$\Gamma(A_2 \rightarrow \pi\gamma) = 0.46 \pm 0.12 \text{ MeV}$$

leads to

$$g^2/4\pi = 0.039 \pm 0.010 \text{ GeV}^{-4}. \quad (8)$$

There exists, however, an independent method—based on VMD—to estimate the value of the coupling constant g . From the well established experimental values¹⁰

$$\Gamma(A_2 \rightarrow \rho\pi) = 71 \pm 3 \text{ MeV}$$

and $f_\rho^2/4\pi \approx 3.0$ one easily obtains

$$g^2/4\pi = (e^2/f_\rho^2)(g_{A\rho\pi}^2/4\pi) \approx 0.07 \text{ GeV}^{-4},$$

which is considerably larger than the more direct

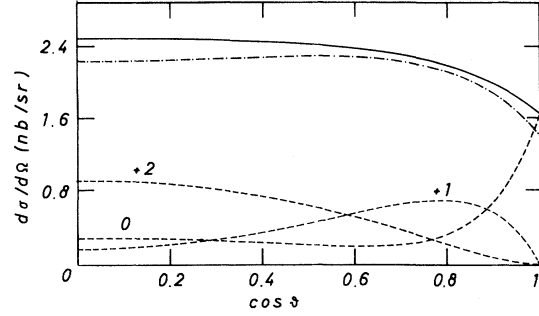


FIG. 2. Differential cross section $d\sigma(\gamma\gamma \rightarrow A_2^\pm \pi^\mp)/d\Omega$ for $W_{\gamma\gamma} = 1.5$ GeV deduced from the amplitude originated by Eq. (2) (solid curve) and by Eq. (9) (dot-dashed curve). Dashed curves stand for the contribution to the differential cross section due to the A_2 helicity states 0, +1 (or -1), and +2 (or -2).

value quoted in Eq. (8). This lower value will be used in all the following computations and, therefore, we feel that this rather conservative procedure could probably represent an underestimate of the effect.

The predictions of our model for the differential cross section $d\sigma(\gamma\gamma \rightarrow A_2\pi)/d\Omega$ for all the final charge states have been plotted (solid line) in Figs. 2 and 3 for center-of-mass energies $W_{\gamma\gamma} = 1.5$ and 1.7 GeV, respectively. The contributions coming from the five helicity states, $\lambda = 0, \pm 1$, and ± 2 , of the final A_2 mesons are also shown (dashed lines). The total cross section has been plotted in Fig. 4 as a function of $W_{\gamma\gamma}$ (solid curve). The dominant contribution to the cross section is due to the contact term, which has also been plotted (dashed curve) in Fig. 4. It is the only term contributing to an s -wave $A_2\pi$ final state and its dominance justifies the approximate isotropy expected for the angular distributions (Figs. 2 and 3).

The most relevant feature of our results is obviously the large values predicted for the cross sections.

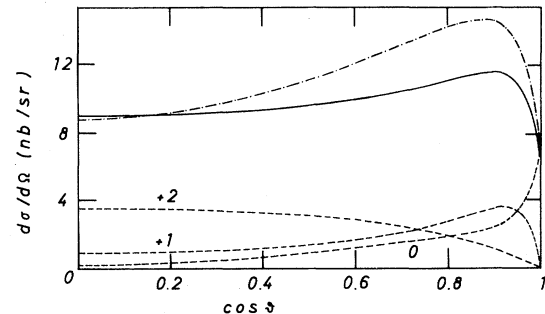


FIG. 3. Differential cross section $d\sigma(\gamma\gamma \rightarrow A_2^\pm \pi^\mp)/d\Omega$ for $W_{\gamma\gamma} = 1.7$ GeV with the same conventions as in Fig. 2.

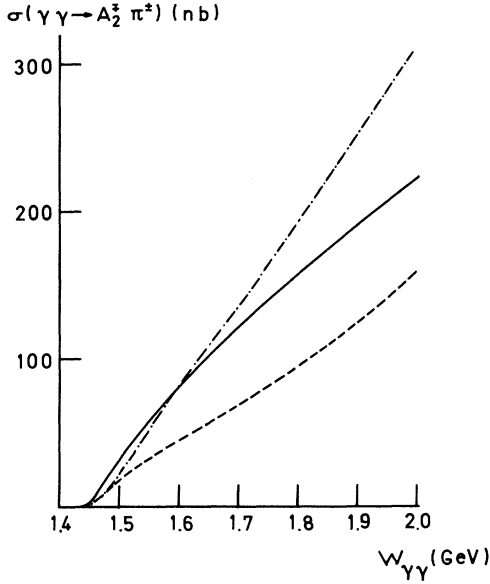


FIG. 4. Total cross section $\sigma(\gamma\gamma \rightarrow A_2^\pm \pi^\mp)$ vs $W_{\gamma\gamma}$. The conventions for the solid and the dot-dashed curves are the same as in Fig. 2. Dashed curve stands for the contribution of the contact term.

Indeed, at $W_{\gamma\gamma} = 1.6, 1.7$ GeV one has

$$\sigma(\gamma\gamma \rightarrow A_2\pi) = 79 \pm 10, 121 \pm 31 \text{ nb}$$

and, taking into account the experimental branching ratio¹⁰ for $A_2^\pm \rightarrow \rho^0 \pi^\pm$,

$$\begin{aligned} \sigma(\gamma\gamma \rightarrow \pi^+\pi^-\pi^+\pi^-) &= \sigma(\gamma\gamma \rightarrow \pi^+\pi^-\pi^0\pi^0) \\ &= 28 \pm 7, 42 \pm 10 \text{ nb} \end{aligned}$$

respectively. As previously stated, absorptive effects are expected to decrease our predictions. However, according to the discussion of Ref. 7, absorption becomes important only for $W_{\gamma\gamma}$ values far from threshold. For this reason (and also because the use of the VMD value for g could still increase our predictions) we have investigated whether these large cross sections are a necessary consequence of our model or can be somehow avoided.

To this end we have replaced the phenomenological Lagrangian leading to the $A_2 \rightarrow \gamma\pi$ matrix element quoted in Eq. (2) by a second one leading to

$$T'(A_2 \rightarrow \pi\gamma) = g \epsilon_{\alpha\beta\gamma\delta} \epsilon'^{\alpha} k'^{\beta} p^{\gamma} \epsilon^{\delta\lambda} q_{\lambda} \quad (9)$$

Obviously, Eqs. (2) and (9) are fully equivalent when describing (on-shell) $A_2 \rightarrow \pi\gamma$ transitions. However, as is often the case when dealing with phenomenological Lagrangians, Eq. (9) leads to a different amplitude for the contact term,

$$T'_{CT} = -eg \epsilon_{\alpha\beta\gamma\delta} (\epsilon'^{\alpha} k'^{\beta} p^{\gamma} \epsilon^{\delta\lambda} \epsilon_{\lambda} - \epsilon'^{\alpha} k'^{\beta} \epsilon^{\gamma} \epsilon^{\delta\lambda} q_{\lambda}) \quad (10)$$

and for T_A ,

$$T'_A = +eg \frac{\epsilon \cdot (k-2p)}{2k \cdot p} \epsilon_{\alpha\beta\gamma\delta} \epsilon'^{\alpha} k'^{\beta} (k-p)^{\gamma} \epsilon^{\delta\lambda} q_{\lambda} \quad (11)$$

Repeating the previous calculations along the same lines with this new gauge-invariant set of amplitudes (10), (4), and (11) leads to the values of the differential and total cross sections (summed for all the A_2 helicity states) plotted in Figs. 2, 3, and 4 (dot-dashed lines). In view of the similarity of the results one has to conclude that the large values of $\sigma(\gamma\gamma \rightarrow A_2\pi)$ are an unavoidable consequence of contact terms.

To some extent, these large values for the $\gamma\gamma \rightarrow A_2\pi$ cross section could have been anticipated from the results of previous work¹¹ on the reaction $\gamma\gamma \rightarrow \rho\pi$, for which rather large and growing cross sections had been similarly predicted. First, because in $\gamma\gamma$ collisions the $\rho\pi$ final state can be produced only in a p wave (or higher), while an s -wave production, generally associated with large threshold enhancements,^{7,8} is fully allowed for an $A_2\pi$ final state. Secondly, because the different (isovector versus isoscalar) nature of the photons involved, respectively, in the A_2 and $\rho \rightarrow \pi\gamma$ vertices tends again to enhance the cross section for $\gamma\gamma \rightarrow A_2\pi$ over that for $\gamma\gamma \rightarrow \rho\pi$ [notice that, accordingly, one knows that¹⁰ $\Gamma(A_2 \rightarrow \pi\gamma)/\Gamma(\rho \rightarrow \pi\gamma) \simeq 7$]. Finally, an independent hint indicating the relevance of contact terms in $\gamma\gamma \rightarrow A_2\pi$ follows from the results of a second work¹² predicting large values (an important fraction of the experimental ones) for $\sigma(\gamma\gamma \rightarrow \rho^0 \pi^+ \pi^- \rightarrow \pi^+ \pi^- \pi^+ \pi^-)$ in a similar context. Indeed, the first step of the latter chain does not contain a genuine (i.e., without propagators) contact term as that of Fig. 1(a) responsible for the large values of $\sigma(\gamma\gamma \rightarrow A_2\pi)$. This compensates the phase-space suppression near threshold due to the large A_2 mass.

A comparison of our global predictions for $\sigma(\gamma\gamma \rightarrow \rho^0 \pi^+ \pi^-)$ with the available data is in order. To this aim one has to observe that the phase of our amplitude for $\gamma\gamma \rightarrow A_2^\pm \pi^\mp \rightarrow \rho^0 \pi^+ \pi^-$ (with on-shell A_2 mesons) and that for $\gamma\gamma \rightarrow \rho^0 \pi^+ \pi^-$ (Ref. 12) differ in 90° . Thus, our global prediction for $\sigma(\gamma\gamma \rightarrow \rho^0 \pi^+ \pi^-)$ can be obtained by simply adding the contributions from these two channels. The results are displayed in Fig. 5. The two upper curves have been obtained from the two amplitudes discussed in this paper and ignoring the effects of absorption. These effects can be estimated by introducing a conventional absorption factor of the form

$$\exp[-(W_{\gamma\gamma} - W_{th})^2/\theta^2]$$

for each channel (where W_{th} is the corresponding threshold and $\theta = 0.8$ GeV has been taken from Ref.

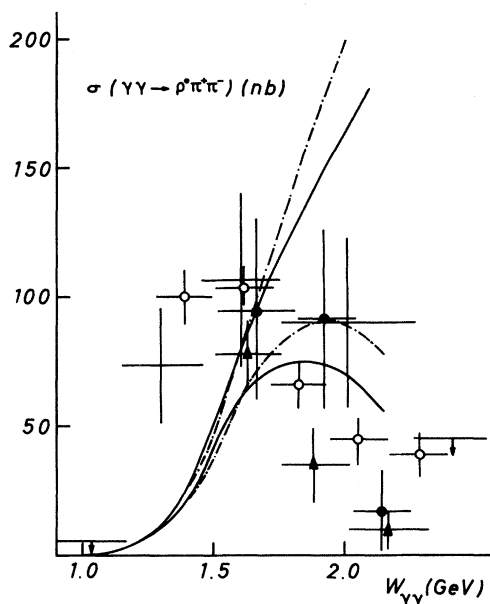


FIG. 5. Total cross section $\sigma(\gamma\gamma \rightarrow \rho^0\pi^+\pi^-)$ vs $W_{\gamma\gamma}$, with the same conventions as in Fig. 2. The two lower (upper) curves include (ignore) absorptive corrections. The experimental data are from TASSO (triangles), Mark II (crosses), CELLO (open dots), and PLUTO (full dots) (Refs. 1, 2, and 3).

13). One then obtains the two lower curves of Fig. 5 showing a rough agreement with the data.

The contact terms discussed in this Brief Report could in principle also be of interest when considering

A_2 -meson decays into $\rho\pi\gamma$ and $\pi\gamma\gamma$ final states along the lines of Ref. 14. However, this does not seem to be the case due to the smallness of our predictions. Indeed, we have estimated the branching ratios of the A_2^\pm meson into $(\rho\pi)^\pm\gamma$ and $\pi^\pm\gamma\gamma$ obtaining 1.1×10^{-4} and 5×10^{-6} , respectively. As in the case of the $A_2 \rightarrow \gamma\gamma$ transition, whose small branching ratio ($\sim 7 \times 10^{-6}$) has been established¹⁰ indirectly through a $\gamma\gamma \rightarrow A_2$ formation experiment, our large predictions for $\sigma(\gamma\gamma \rightarrow A_2^\pm\pi^\mp)$ imply small values for the $A_2 \rightarrow \rho\pi\gamma$ and $\pi\gamma\gamma$ decay widths. The corresponding branching ratios have not been measured and, unfortunately, seem to escape the present possibilities of a direct detection.

Therefore, it seems reasonable to conclude that the transition $\gamma\gamma \rightarrow A_2^\pm\pi^\mp \rightarrow \rho^0\pi^+\pi^-$ should present an important threshold enhancement due to a contact interaction in its first step. A very substantial fraction of the large cross section for $\gamma\gamma \rightarrow \pi^+\pi^-\pi^+\pi^-$ observed at PETRA and SPEAR for $W_{\gamma\gamma} = 1.4$ –2 GeV, i.e., just above the $A_2\pi$ threshold, could be attributed to this mechanism, especially, if the $A_2\pi\gamma$ coupling constant is taken from the well-established $A_2 \rightarrow \rho\pi$ decay width and VMD. Then, the contributions to the $\gamma\gamma \rightarrow \pi^+\pi^-\pi^+\pi^-$ cross section coming from our simple contact-term mechanism for the $A_2\pi$ channel, together with those of Ref. 12 for the $\rho^0\pi^+\pi^-$ one, could easily account for the whole experimentally observed effect with no need of new speculative contributions.^{4–6} The observation or not of the A_2^\pm resonance peak in the $(\rho\pi)^\pm$ invariant-mass spectrum will represent a crucial test for our approach.

¹R. Brandelik *et al.*, Phys. Lett. **97B**, 448 (1980).

²D. L. Burke *et al.*, Phys. Lett. **103B**, 153 (1981).

³CELLO Collaboration, contributed paper to International Conference on High Energy Physics, Lisbon, 1981 (unpublished); J. H. Field, in *Proceedings of the 4th International Colloquium on Photon-Photon Interactions, Paris, 1981*, edited by G. W. London (World Scientific, Singapore, 1981); A. Courau, in *Proceedings of the 3rd Seminar on $\gamma\gamma$ Physics, Orsay, 1981* (Laboratoire de l'Accélérateur Lineaire, Orsay, 1982).

⁴H. Goldberg and T. Weiler, Phys. Lett. **102B**, 63 (1981).

⁵J. Layssac and F. M. Renard, Montpellier Report No. PM/80/11, 1980 (unpublished); R. M. Godbole and K. V. L. Sarma, Phys. Lett. **109B**, 504 (1982).

⁶B. A. Li and K. F. Liu, Report No. SLAC-PUB-2783, 1981 (unpublished).

⁷D. Lüke and P. Söding, in *Springer Tracts in Modern Physics Vol. 59*, edited by G. Höhler (Springer, Berlin, 1971), p. 39.

⁸P. Stichel and M. Scholz, Nuovo Cimento **34**, 1381 (1964); P. V. Collins, H. Kowalski, H. Römer, and H. R. Rubinstein, Phys. Lett. **44B**, 183 (1973).

⁹G. Carbone, Nuovo Cimento **58A**, 23 (1968).

¹⁰Particle Data Group, Phys. Lett. **111B**, 1 (1982).

¹¹E. Bagán, A. Bramon, and F. Cornet, Phys. Rev. D **25**, 2306 (1982).

¹²C. Ayala, A. Bramon, and F. Cornet, Phys. Lett. **107B**, 235 (1981).

¹³C. Ferro Fontan and H. R. Rubinstein, Nucl. Phys. **B74**, 378 (1974); Y. Goldschmidt and H. R. Rubinstein, *ibid.* **B97**, 445 (1975).

¹⁴A. Bramon and F. Cornet, Phys. Lett. **83B**, 235 (1979).